

Direct Torque Control Strategy (DTC) Based on Fuzzy Logic Controller for a Permanent Magnet Synchronous Machine Drive

A. Tlemcani[†], O. Bouchhida*, K. Benmansour**, D. Boudana* and M. S. Boucherit*

Abstract – This paper introduces the design of a fuzzy logic controller in conjunction with direct torque control strategy for a Permanent Magnet synchronous machine. A stator flux angle mapping technique is proposed to reduce significantly the size of the rule base to a great extent so that the fuzzy reasoning speed increases. Also, a fuzzy resistance estimator is developed to estimate the change in the stator resistance. The change in the steady state value of stator current for a constant torque and flux reference is used to change the value of stator resistance used by the controller to match the machine resistance.

Keywords: Direct torque control, fuzzy logic, fuzz resistance estimator, permanent magnet synchronous machine drive, stator resistance, switching tables

1. Introduction

Permanent magnet synchronous motors (PMSM) are widely used in high-performance drives such as industrial robots and machine tools thanks to their known advantages of: high power density, high-torque/inertia ratio, and free maintenance. In recent years, the magnetic and thermal capabilities of the PMSM have been considerably increased by employing high-coercive PMSM materials. The Direct Torque Control (DTC) method was first proposed for induction machines in the mid-1980s (Takahashi and Noguchi [1], [2], Depenbrock), and then extended to PMSM motors [3], [4]. This technique is becoming more and more accepted nowadays since the basic idea of DTC for motors is to control the torque and flux linkage by selecting the voltage space vectors properly, which is based on the relationship between the slip frequency and torque.

In the late 1990s, DTC techniques for PMSM machines have appeared [5], [3]. Figure 1 shows a DTC system for an Interior Permanent Magnet motor. It is seen that no extra sensors are needed to implement DTC when compared with vector control except for the use of a voltage sensor. The rotor position, which is essential for torque control in a vector control scheme, is not required in DTC provided the initial rotor position is known. This makes the sensorless PMSM drive easier to implement [6].

Basically, direct torque control employs two hysteresis controllers to regulate the stator flux and the torque respectively, which results in approximate decoupling between the flux and the torque control. The key issue of designing the DTC lies in the strategy of how to choose a proper stator voltage vector to keep the stator flux and the torque in their prescribed band [7].

In most DTC schemes, a hysteresis controller is used. The latter is usually a two-value bang-bang type controller, which naturally leads to taking the same action for the big torque error and the small one. As a consequence, the above scheme gives poor performances in response to step changes and large torque ripple. In order to improve the performance of the DTC, it is natural to divide the torque error into several intervals on which different control action is taken; since the DTC control strategy is not based on a motor mathematical model, it is not easy to give an apparent boundary to the division of the torque error.

Besides, fuzzy control is a way of controlling a system without knowing its mathematic model and which uses the experience of people knowledge to form its control rule base. Many applications of fuzzy control have appeared in power electronics and drive controls in the past few years [8]. A fuzzy logic controller was reported in [9] being used with DTC [10]. However, there arises the problem that the rule numbers used is very large (180 rules) and will slow down the speed of the fuzzy reasoning.

This paper introduces the design of a fuzzy logic controller in conjunction with a direct torque control strategy for a Permanent Magnet synchronous machine. A stator flux angle mapping technique is proposed to reduce significantly the size of the rule base to a great extent so that the fuzzy reasoning speed increases. Also, a fuzzy resistance estimator is developed to estimate the change in the stator resistance. The

[†] Corresponding Author: Laboratoire de Commande des Processus, Département du Génie Electrique, Ecole Nationale Polytechnique, 10, ave Hassen Badi, BP. 182, El-Harrach, Alger, Algérie (h.tlemcani@yahoo.fr)

* Laboratoire de Commande des Processus, Département du Génie Electrique, Ecole Nationale Polytechnique, 10, ave Hassen Badi, BP. 182, El-Harrach, Alger, Algérie

** Equipe Commande des Systèmes, ENSEA., 95014 Cergy-Pontoise Cedex, France (benmansour@ensea.fr)

Received 14 April, 2008 ; Accepted 29 January, 2009

change in the steady state value of stator current for a constant torque and flux reference is used to change the value of stator resistance used by the controller to match the machine resistance.

The paper is organized as follows. In section 2, the PMSM motor model is discussed. In section 3, the DTC scheme is given. The fuzzy controller is proposed in section 4, where three approaches for the optimization of fuzzy rules are discussed. Section 5 is devoted to the stator resistance estimator which is based on fuzzy logic

2. Mathematical model of PMSM

The electrical and mechanical equations of the PMSM motor in the rotor d-q reference frame can be expressed as:

$$\begin{aligned} v_d &= R_s i_d + L_d \frac{di_d}{dt} - pL_q \Omega i_q \\ v_q &= R_s i_q + L_q \frac{di_q}{dt} + pL_d \Omega i_d + p\Omega \Phi_f \end{aligned} \quad (1)$$

$$\begin{aligned} J \frac{d\Omega}{dt} &= T_{em} - T_r - F_c \Omega \\ T_{em} &= \frac{P|\Phi_s|}{2L_d L_q} [2\Phi_f L_q \sin \gamma - |\Phi_s| (L_q - L_d) \sin 2\gamma] \end{aligned} \quad (2)$$

Where:

R_s : Stator armature resistance;

L_d, L_q : Direct and quadrature inductance;

Ω : Rotor speed;

p : Pole pairs;

v_d, v_q : Stator voltage in d-q-axis;

i_d, i_q : Stator current in d-q-axis;

Φ_f : Flux created by the rotor magnets;

Φ_s : Stator flux;

T_{em}, T_r : Electromagnetic torque and load torque;

F_c : Viscous friction coefficient;

J : Total moment of inertia of the motor and load;

γ : Angle between rotor and stator flux linkage;

The state vector is composed by the (d-q) current components (i_d, i_q), and the rotor speed Ω , whereas a vector control is composed of the rotor voltage components (v_d, v_q) and the external disturbance is represented by the load torque T_r [3]. Under the condition of constant amplitude of Φ_s , by differentiating equation (2) with respect to time, the rate of increasing of torque can be obtained.

$$\frac{dT_{em}}{dt} = \frac{P|\Phi_s|}{2L_d L_q} [2\Phi_f L_q \dot{\gamma} \cos \gamma - 2|\Phi_s| (L_q - L_d) \dot{\gamma} \cos 2\gamma] \quad (3)$$

The derivative of torque is always positive provided that γ is within the range of $[-\pi/2, \pi/2]$ which implies that the increase of torque is proportional to the increase of angle γ . In other words, the stator flux linkage should be controlled in such a way that flux amplitude is kept constant and the rotating speed is controlled as fast as possible to obtain the maximum change in actual torque [12]. Therefore, for PMSMs, the amplitude of the stator flux linkage should also be changed with the change of actual torque for maintaining a positive $dT/d\gamma$.

With constant stator flux linkage, the condition for positive $dT/d\gamma$ around $\gamma=0$ is given by:

$$|\Phi_s| < \frac{L_q}{L_q - L_d} \Phi_f \quad (4)$$

By differentiating (2) with respect to γ and equalizing it to zero, the condition for maximum allowable angle γ_m can be found, as:

$$\gamma_m = \cos^{-1} \left\{ \frac{a/|\Phi_s| - \sqrt{(a/|\Phi_s|)^2 + 8}}{4} \right\} \quad (5)$$

Where:

$$a = \frac{\Phi_f L_q}{L_q - L_d}$$

In maintaining positive $dT_{em}/d\gamma$ the torque angle γ should be also controlled to not exceed γ_m which is corresponding to the maximum torque [11]. Hence, the application of DTC in PMSM drives, the amplitude of the stator flux linkage should be controlled to satisfy (4), and γ must also be limited to γ_m .

3. Implementation of DTC for a PMSM Drive

The DTC scheme for a PMSM drive is shown in Fig. 1.

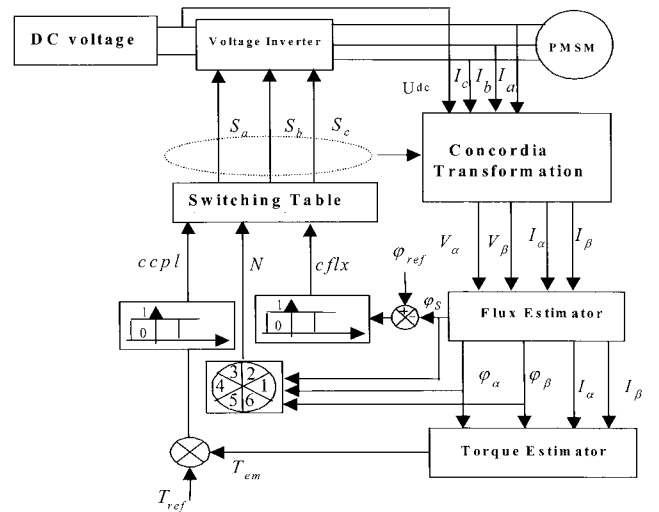


Fig. 1. DTC scheme for PMSM drive

3.1 Control Algorithm

Between switching intervals, each voltage vector is constant and the stator flux linkage of a PMSM can be expressed in the stationary reference frame as:

$$\varphi_s = V_s t - R \int I_s dt + \varphi_s|_{t=0} \tag{6}$$

Neglecting the stator resistance, (6) implies that the tip of the stator flux vector, φ_s will move in the direction of the applied voltage vector. $\varphi_s|_{t=0}$ is the initial stator flux linkage at the instant of switching. To select the voltage vectors for controlling the amplitude of φ_s , the voltage vector plane is divided into six regions. In each region, two adjacent voltage vectors, which give the minimum switching frequency, are selected to increase or decrease the amplitude φ_s respectively [5].

The torque increases with the angle, not with the slip frequency as in induction motors. For controlling the amplitude of the stator flux linkage and for changing the torque or angle quickly, zero voltage vectors are not used in PMSM. For induction motors, the application of zero voltage vectors immediately makes the slip frequency and torque negative. For PMSMs, the change of torque must occur through change in angle. The application of zero voltage vectors will make this change subject to the rotor mechanical time constant which can be rather long. In other words, φ_s should always be in motion with respect to the rotor flux linkage. The rotating direction of φ_s is determined by the output of the torque controller.

3.2 Hysteresis Controller

Let the stator flux space vector be located in the k sector ($k=1,2,\dots,6$) of the d - q plane as drawn in Fig. 2. In order to increase the amplitude of the stator flux, the inverter voltage space vectors V_k, V_{k+1}, V_{k-1} should be applied to the motor. Conversely, to decrease its amplitude, $V_{k+2}, V_{k-2}, V_{k+3}$ must be applied.

The inverter voltage utilized for the control of the stator flux amplitude acts also on the motor torque. From the previous section, it turns out that inverter voltage space vectors which cause an increase in the slip speed of the stator flux produce a torque increase. The converse is true for the space vectors which reduce the slip speed of the stator flux [13], [14].

Table 1 summarizes the combined action of each inverter voltage space vector on both the stator flux amplitude and the motor torque. In this table, a single arrow means a small variation, whereas two arrows mean a larger variation. As it appears from the table, an increment of torque (\uparrow) is obtained by applying the space vectors V_{k+1} and V_{k+2} , irrespective of the motor speed direction. Conversely, a decrement of

torque (\downarrow) is obtained by applying V_{k-1} or V_{k-2} . The space vectors V_k, V_{k+3} and the zero voltage space vectors alter the torque in accordance with the motor speed direction as specified in Table 1.

Table 1. Combined action of each inverter voltage space vector V_i

	V_{i-2}	V_{i-1}	V_i	V_{i+1}	V_{i+2}	V_{i+3}	v_0, v_7
φ_s	\downarrow	\uparrow	$\uparrow\uparrow$	\uparrow	\downarrow	$\downarrow\downarrow$	$\downarrow\uparrow$
$T_{em} (\Omega > 0)$	$\downarrow\downarrow$	$\downarrow\downarrow$	\downarrow	\uparrow	\uparrow	\downarrow	\downarrow
$T_{em} (\Omega < 0)$	\downarrow	\downarrow	\uparrow	$\uparrow\uparrow$	$\uparrow\uparrow$	\uparrow	\uparrow

Table 2. Four switching solutions

	$T_{em} \uparrow \varphi_s \uparrow$	$T_{em} \uparrow \varphi_s \downarrow$	$T_{em} \downarrow \varphi_s \uparrow$	$T_{em} \downarrow \varphi_s \downarrow$
1 st Switching	V_{i+1}	V_{i+2}	v_0, v_7	v_0, v_7
2 nd Switching	V_{i+1}	V_{i+2}	V_i	v_0, v_7
3 rd Switching	V_{i+1}	V_{i+2}	V_i	V_{i+3}
4 th Switching	V_{i+1}	V_{i+2}	V_{i-1}	V_{i-2}

With hysteresis controllers having a two level output, there are four conditions regarding the stator flux and the motor torque voltage demands. For each condition it can be found at least one inverter voltage space vector which acts in the way of reducing the error signals. This demonstrates that a voltage inverter is able to regulate in a direct manner the stator flux amplitude and the motor torque of a PMSM or to force them so as to track any reference.

Several switching solutions can be employed to control the torque according to whether the stator flux has to be reduced or increased. Each solution influences the drive behavior in terms of torque and current ripple, switching frequency, and two- or four-quadrant operation capability. In Table 2 four switching solutions are given. Upon each solution, a switching table can be built and implemented in the block selector of Fig. 2. The switching table inputs are the two-level demands of stator flux and torque, and the stator flux sector, whilst the switching table output is the inverter voltage space vector for the motor [14].

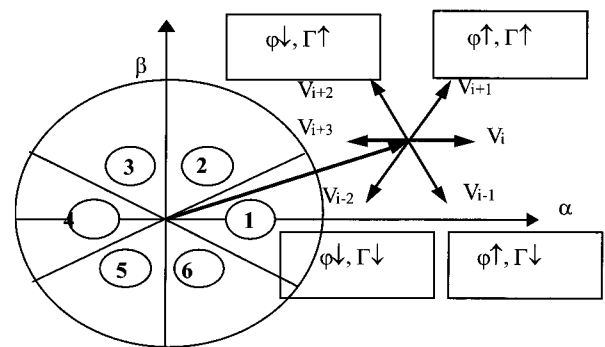


Fig. 2. Inverter voltage and corresponding stator flux variations

To use the switching table, rather than the position of the flux, the zone where the flux is situated is used. In the tables, Cflx and ccpl are the outputs of the hysteresis controllers for flux linkage and torque, respectively.

The flux linkage N ($N=1: 6$), where N indicates the situation of the flux position, can be obtained by the following equations:

$$(2N - 3)\pi/6 < \theta < (2N - 1)\pi/6 \quad (7)$$

Fig. 3. gives flux trajectories for different switching strategies, the most circular trajectories are given in Table 5 and Table 6.

One can see the hard trajectory oscillations in Table 5. The torque responses to the different switching algorithms are given in Fig. 4.

One can see the hard trajectory oscillations in Table 5. The torque responses to the different switching algorithms are given in Fig. 4. Table 3 gives the best performance with respect to Tables 4, 5 and 6. The latter exhibits hard torque oscillations. The same conclusions for the currents responses can be obtained from Fig. 5.

Table 3. The 1st switching strategy

Torque	Flux	N=1	N=2	N=3	N=4	N=5	N=6
ccpl = 1	Cflx = 1	V ₂	V ₃	V ₄	V ₅	V ₆	V ₁
	Cflx = 0	V ₃	V ₄	V ₅	V ₆	V ₁	V ₂
ccpl = 0	Cflx = 1	V ₇	V ₀	V ₇	V ₀	V ₇	V ₀
	Cflx = 0	V ₀	V ₇	V ₀	V ₇	V ₀	V ₇

Table 4. The 2nd switching strategy

Torque	Flux	N=1	N=2	N=3	N=4	N=5	N=6
ccpl = 1	Cflx = 1	V ₂	V ₃	V ₄	V ₅	V ₆	V ₁
	Cflx = 0	V ₃	V ₄	V ₅	V ₆	V ₁	V ₂
ccpl = 0	Cflx = 1	V ₁	V ₂	V ₃	V ₄	V ₅	V ₆
	Cflx = 0	V ₀	V ₇	V ₀	V ₇	V ₀	V ₇

Table 5. The 3rd switching strategy

Torque	Flux	N=1	N=2	N=3	N=4	N=5	N=6
ccpl = 1	Cflx = 1	V ₂	V ₃	V ₄	V ₅	V ₆	V ₁
	Cflx = 0	V ₃	V ₄	V ₅	V ₆	V ₁	V ₂
ccpl = 0	Cflx = 1	V ₁	V ₂	V ₃	V ₄	V ₅	V ₆
	Cflx = 0	V ₄	V ₅	V ₆	V ₁	V ₂	V ₃

Table 6. The 4th switching strategy

Torque	Flux	N=1	N=2	N=3	N=4	N=5	N=6
ccpl = 1	Cflx = 1	V ₂	V ₃	V ₄	V ₅	V ₆	V ₁
	Cflx = 0	V ₃	V ₄	V ₅	V ₆	V ₁	V ₂
ccpl = 0	Cflx = 1	V ₆	V ₁	V ₂	V ₃	V ₄	V ₅
	Cflx = 0	V ₅	V ₆	V ₁	V ₂	V ₃	V ₄

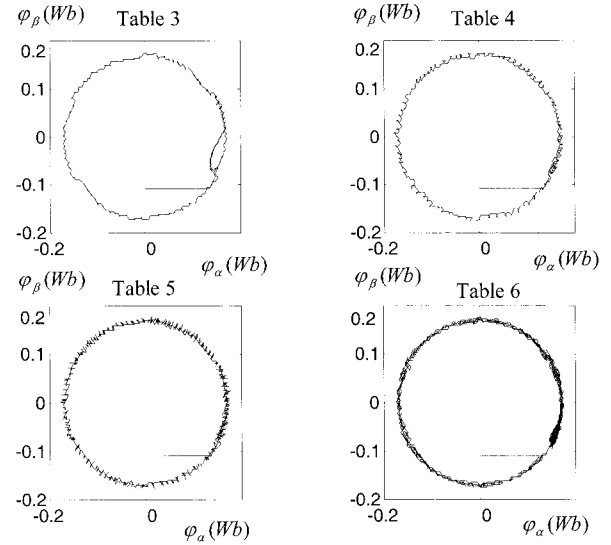


Fig. 3. Flux trajectories for different switching strategies

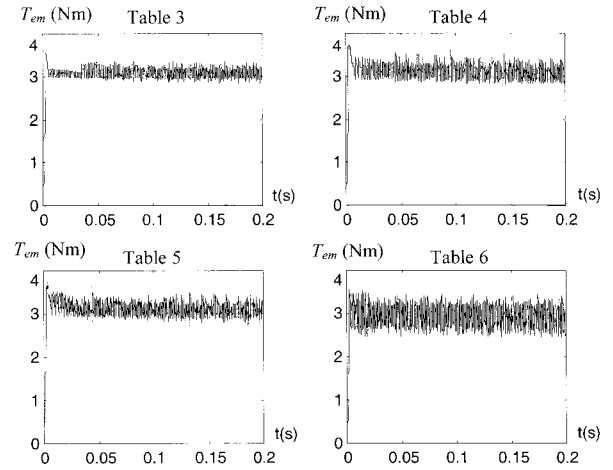


Fig. 4. Torque responses to the different switching algorithms

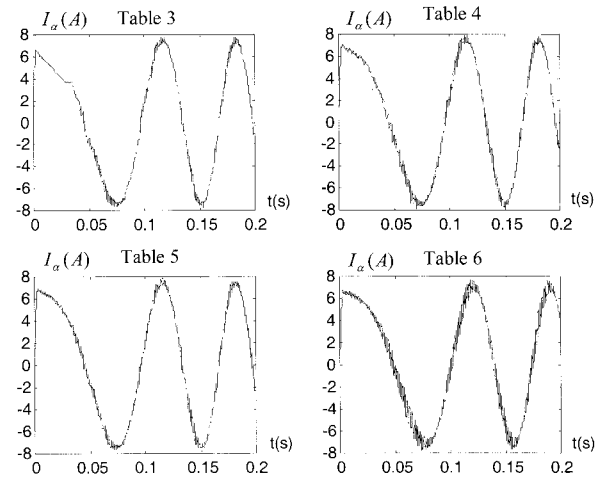


Fig. 5. Currents responses to the different switching algorithms

The case of inverting the torque is given in Fig. 6. One can see that the inversion of the torque fails with strategies of

Tables 3, 4 and 5. However, with the strategy of Table 6, the inversion is done and a good response is obtained.

In the sequel we will use only Table 6 for the simulations since it gives the best compromise between flux and torque.

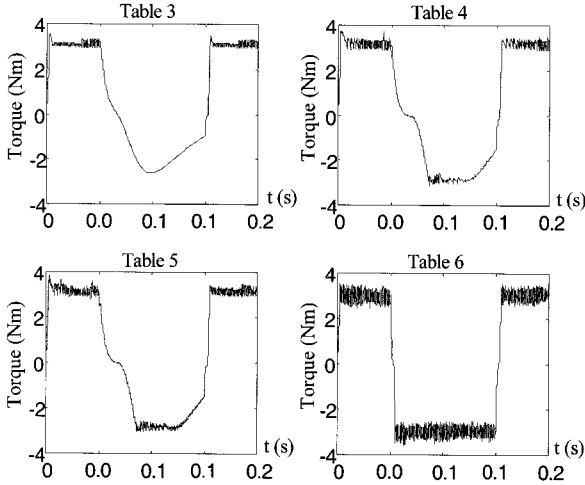


Fig. 6. Inverting the torque to the different switching algorithms

4. Fuzzy logic controller

From the discussion in the previous section the controller adopting DTC strategy is a type of hysteresis, which means the control action will be the same in the whole error range.

To obtain better control effect a fuzzy logic controller has been introduced to replace the hysteresis controller. The diagram of a direct torque control incorporated with a fuzzy logic controller is shown in Fig. 7. Generally speaking, a fuzzy logic controller consists of three main parts: fuzzification, fuzzy reasoning and defuzzification. We will discuss three approaches: the first approach developed [16] was for induction motors and adopted by us for PMSM; the second was developed by [21]; and the third approach is proposed in this paper.

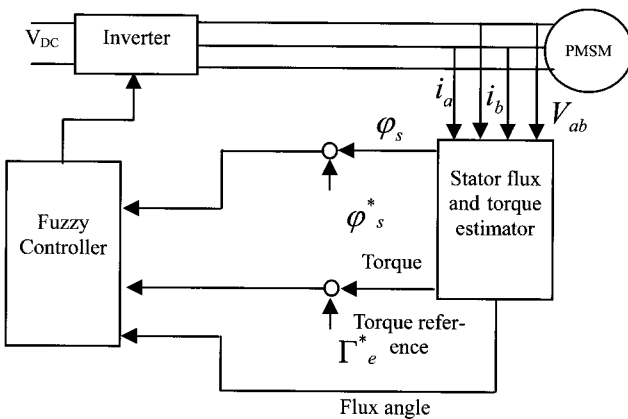


Fig. 7. Fuzzy controller for direct torque control of PMSM

4.1 First Approach

4.1.1 Fuzzy state and control variables

The fuzzification is the process of a mapping from measured or estimated input to the corresponding fuzzy set in the input universe of discourse. In this system there are three inputs, which are E_φ (error of stator flux), E_{T_e} (error of torque) and θ (stator flux angle) respectively. They are defined as:

$$\begin{aligned} E_\varphi &= \varphi_s^* - |\varphi_s| \\ E_{T_e} &= T_e^* - T_e \\ \theta &= \text{tg}^{-1}\left(\frac{\varphi_\beta}{\varphi_\alpha}\right) \end{aligned} \quad (8)$$

Where φ_s^* and T_e^* are references of stator flux and torque respectively, φ_s is the magnitude of stator flux, which can be estimated.

The fuzzification is performed using membership function with a singleton fuzzifier. There are three groups of membership function depicted in Fig. 8 corresponding to three input variables. The universe of discourse of fuzzy angle variable is divided into 12 fuzzy sets θ_1 to θ_{12} . The control variable is the inverter switching state (N). In a six step inverter, seven distinct switching states are possible [18]. The switching states are crisp thus do not need a fuzzy membership distribution.

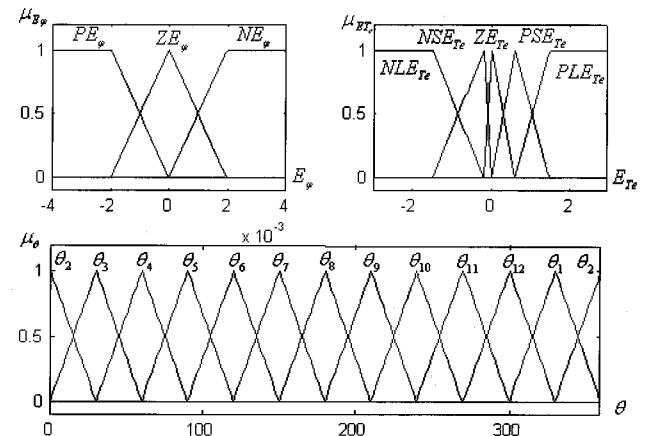


Fig. 8. Membership distribution of fuzzy variables for first approach

4.1.2 Fuzzy rules for self control

Each control rule can be described using the state variables E_φ , E_{T_e} and θ and the control variable N. The rule R_i can be written as:

$$R_i : \text{if } E_\phi \text{ is } A_i, E_{T_e} \text{ is } B_i \text{ and } \theta \text{ is } C_i \text{ then } N \text{ is } N_i \quad (9)$$

Where A_i , B_i , C_i and N_i represent the fuzzy segments.

The control rules are formulated using the vector diagram for direct self control as shown in Fig. 9.

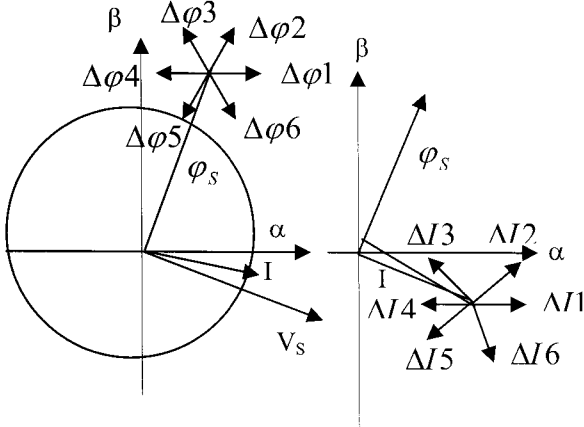


Fig. 9. Vector diagram used for knowledge base

Looking at the position of the flux in Fig. 9 states 5, 6 and 1 will increase the flux while states 2, 3 and 4 will decrease it. Similarly states 6, 1 and 2 will increase the torque while states 3, 4 and 5 will decrease it. For a large increase in flux and a small increase in torque, state 6 is selected. For a small increase in flux and a large increase in torque, state 1 is selected. For a small decrease in flux and a small increase in torque, state 2 is selected. For a large decrease in flux and a small decrease in torque, state 3 is selected. For a small decrease in flux and a large decrease in torque, state 4 is selected. For a small increase in flux and a large decrease in torque, state 5 is selected. For a small decrease in torque and constant flux, state 0 is selected. This selection changes as the position of the flux vector changes. The total number of rules is 180 as shown in Table 5. Each cell in this diagram shows the best switching state for the given angle.

The total number of obtained rules is 132 instead of 180 obtained in [16] since we do not use the null voltage vectors for DTC in the PM motors. The latter's are represented in the 12 tables shown below Tab. 7. Each table gives the best switch state for a given flux angle.

4.1.3 Fuzzy Interface

The interface method used is basic and simple and is developed from the minimum operation rule as a fuzzy implementation function [19]. The membership functions of A , B , C and N are given by μ_A , μ_B , μ_C and μ_N respectively. The firing strength of i^{th} rule α_i can be expressed as:

$$\alpha_i = \min(\mu_{A_i}(E_\phi), \mu_{B_i}(E_{T_e}), \mu_{C_i}(\theta)) \quad (10)$$

By fuzzy reasoning using Mamdani's minimum operation rule as a fuzzy implication function, the i^{th} rule leads to the control decision:

$$\mu_{N_i}(n) = \min(\alpha_i, \mu_{N_i}(n)) \quad (11)$$

Thus the membership function μ_N of the output n is point wise given by:

$$\mu_N(n) = \max_{i=1}^{132}(\mu_{N_i}(n)) \quad (12)$$

Since the output is crisp, the maximum criterion method is used for defuzzification. By this method, the value of fuzzy output which has the maximum possibility distribution is used as the control output.

4.2 Second Approach

In [16] the flux angle has 12 fuzzy subsets which results in 180 rules in the rule base. This is too many to be incorporated into the fuzzy logic Toolbox and is difficult to implement in practice as well. For the purpose of reducing the total rule numbers the input to the fuzzy controller in our case only covers the partial universe $[-\frac{\pi}{6}, \frac{\pi}{6}]$ not like that of $[0, 2\pi]$ which covers the whole universe of discourse [10].

Based on the symmetry of impressed PMW voltage vectors and flux angle in d-q coordinate, we define a mapping to convert the θ in the range of $[0, 2\pi]$ into a sector with range of $[-\frac{\pi}{6}, \frac{\pi}{6}]$:

$$\theta = \theta' - \frac{\pi}{3} \text{Fix} \left[\frac{\theta' + \pi/6}{\pi/3} \right] \quad (13)$$

Where θ is the angle that goes into the fuzzy logic controller.

The operator Fix denotes rounding the variable to the nearest inferior integer. It should be noted here after the fuzzy reasoning that the result action should be converted to the correct voltage vector according to the real angle of the flux.

The control variable obtained by the fuzzy controller is then transformed to the correct value by taking into account the number of the stator flux sector [21].

The Universe of discourse for the new fuzzy variable is divided into 3 fuzzy sets $(\theta_1, \theta_2, \theta_3)$ as shown in Fig. 10.

Using 3 fuzzy sets for the flux angle, we had an incomplete table of 33 rules reported in Table 6.

Table 7. Set of fuzzy rules for first approach

θ_1			
$\begin{matrix} E_{\phi} \\ E_{Te} \end{matrix}$	P	Z	N
PL	1	2	2
PS	1	2	3
ZE	-	-	-
NS	6	-	4
NL	6	5	5

θ_2			
$\begin{matrix} E_{\phi} \\ E_{Te} \end{matrix}$	P	Z	N
PL	2		3
PS	2	3	3
ZE	-	-	-
NS	6	-	5
NL	6	6	5

θ_3			
$\begin{matrix} E_{\phi} \\ E_{Te} \end{matrix}$	P	Z	N
PL	2	3	3
PS	2	3	4
ZE	-	-	-
NS	1	-	5
NL	1	6	6

θ_4			
$\begin{matrix} E_{\phi} \\ E_{Te} \end{matrix}$	P	Z	N
PL	3	3	4
PS	3	4	4
ZE	-	-	-
NS	1	-	6
NL	1	1	6

θ_5			
$\begin{matrix} E_{\phi} \\ E_{Te} \end{matrix}$	P	Z	N
PL	3	4	4
PS	3	4	5
ZE	-	-	-
NS	2	-	6
NL	2	1	1

θ_6			
$\begin{matrix} E_{\phi} \\ E_{Te} \end{matrix}$	P	Z	N
PL	4	4	5
PS	4	5	5
ZE	-	-	-
NS	2	-	1
NL	2	2	1

θ_7			
$\begin{matrix} E_{\phi} \\ E_{Te} \end{matrix}$	P	Z	N
PL	4	5	5
PS	4	5	6
ZE	-	-	-
NS	3	-	1
NL	3	2	2

θ_8			
$\begin{matrix} E_{\phi} \\ E_{Te} \end{matrix}$	P	Z	N
PL	5	5	6
PS	5	6	6
ZE	-	-	-
NS	3	-	2
NL	3	3	2

θ_9			
$\begin{matrix} E_{\phi} \\ E_{Te} \end{matrix}$	P	Z	N
PL	5	6	6
PS	5	6	1
ZE	-	-	-
NS	4	-	2
NL	4	3	3

θ_{10}			
$\begin{matrix} E_{\phi} \\ E_{Te} \end{matrix}$	P	Z	N
PL	6	6	1
PS	6	1	1
ZE	-	-	-
NS	4	-	3
NL	4	4	3

θ_{11}			
$\begin{matrix} E_{\phi} \\ E_{Te} \end{matrix}$	P	Z	N
PL	6	1	1
PS	6	1	2
ZE	-	-	-
NS	5	-	3
NL	5	4	4

θ_{12}			
$\begin{matrix} E_{\phi} \\ E_{Te} \end{matrix}$	P	Z	N
PL	1	1	2
PS	1	2	2
ZE	-	-	-
NS	5	-	4
NL	5	5	4

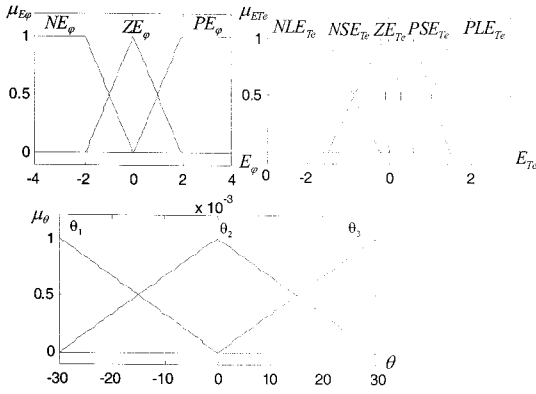


Fig. 10. Membership distribution of fuzzy variables for second approach

Table 8. Set of fuzzy rules for second approach

θ_1				θ_2			
E_ϕ / E_{Te}	P	Z	N	E_ϕ / E_{Te}	P	Z	N
PL	2	2	3	PL	3	3	4
PS	1	2	3	PS	2	3	4
ZE	-	-	-	ZE	-	-	-
NS	6	-	4	NS	1	-	5
NL	6	5	4	NL	6	6	5

θ_3			
E_ϕ / E_{Te}	P	Z	N
PL	2	3	3
PS	1	3	4
ZE	-	-	-
NS	6	-	5
NL	6	6	5

The fuzzy reasoning used is mandani's method Mamdani [9].

$$\alpha_i = \min(\mu_{A_i}(E_\phi), \mu_{B_i}(E_{Te}), \mu_{C_i}(\theta))$$

$$\mu_{N_i}(n) = \min(\alpha_i, \mu_{N_i}(n))$$

$$\mu_N(n) = \max_{i=1}^{33}(\mu_{N_i}(n))$$
(14)

The relation giving the number of the sector in which the stator flux vector lies is obtained as:

$$S = \text{Fix}\left(\left(\frac{\theta + \pi/6}{\pi/3} + 1\right)\right)$$
(15)

We add to the fuzzy regulator output (S-1) in order to get

the correct voltage vector of the inverter configuration.

4.3 Proposed Approach

It is possible to reduce the size of the precedents rules table by using the symmetry of rules table given in the first approach Table 5 and a heuristic repartition of the state flux angle. We see from Table 5 that we can use only 2 fuzzy sets for the flux angle θ (θ_1 and θ_2). This allows eliminating redundancy existing in the fuzzy rules. We have also developed an interesting technique to reduce the number of rules to 22. The third fuzzy controller input (flux angle) actually cover the universe $[0, \frac{\pi}{6}]$ and not $[0, 2\pi]$ as in the first approach.

Based on the symmetry of the voltage vector and the stator flux angle, we define the following transformation that converts the angle θ' from $[0, 2\pi]$ to angle θ in $[0, \frac{\pi}{6}]$:

$$\theta = \text{rem}(\theta')$$
(16)

Where θ is the input angle of the fuzzy controller.

The operator rem used above stands for "remain of division".

Table 9. Set of fuzzy rules for proposed approach

θ_1				θ_2			
E_ϕ / E_{Te}	P	Z	N	E_ϕ / E_{Te}	P	Z	N
PL	1	2	2	PL	1	1	2
PS	1	2	3	PS	1	2	2
ZE	-	-	-	ZE	-	-	-
NS	0	-	4	NS	5	-	4
NL	0	5	5	NL	5	5	4

By using 2 fuzzy sets for flux angle, we obtain 22 rules given in Table 7. Fig. 11 represents the distribution of the underlying fuzzy sets.

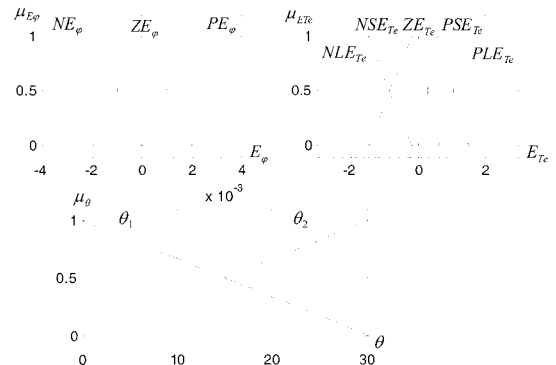


Fig. 11. Membership distribution of fuzzy variables for proposed approach

4.4 Simulation of the System

To study the performance of the fuzzy logic controller with the direct torque control strategy, the system simulation was conducted using Matlab and a fuzzy logic toolbox. The parameters of the motor are given in Table 10.

Table 10. Parameters of the used motor

Nombre of pole pairs	P	2
Armature resistance	R_s	0.57 Ω
Magnet flux linkage	Φ_f	0.108 Wb
d-axis Inductance	L_d	8.72 mH
q-axis Inductance	L_q	22.8 mH
Phase voltage	V	50 V
Phase current	I	8.66 A
Base speed	Ω	1200 rpm

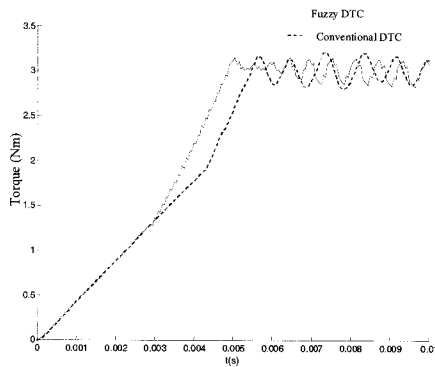


Fig. 12. Torque response of fuzzy controller and conventional DTC during start-up

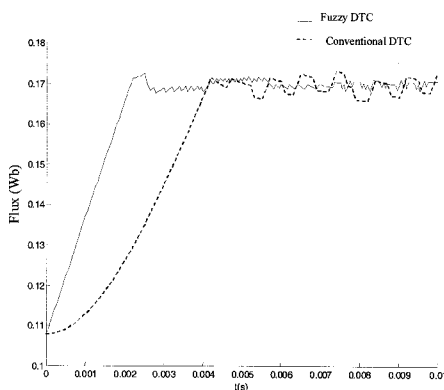


Fig. 13. Stator flux response of fuzzy controller and conventional DTC during start-up

Fig. 12 and 13 shows the torque and the stator flux responses of the system during start-up for the conventional DTC and the fuzzy controller. The response of the fuzzy controller is faster than the conventional DTC. In the fuzzy controller the initial stator flux error is very large. Thus the controller chooses the states giving a higher increase in the flux. The change in torque during this time is small. Once the flux error becomes small, the controller chooses the states giving

a faster increase in torque.

Fig. 14 shows the response of the system for a step change in torque from 3Nm to 1Nm keeping the flux command constant. The response of the fuzzy controller is faster than the conventional controller.

The steady state torque and flux vector in Fig. 15 and Fig. 16 shows nearly a circular path indicating a good flux regulation.

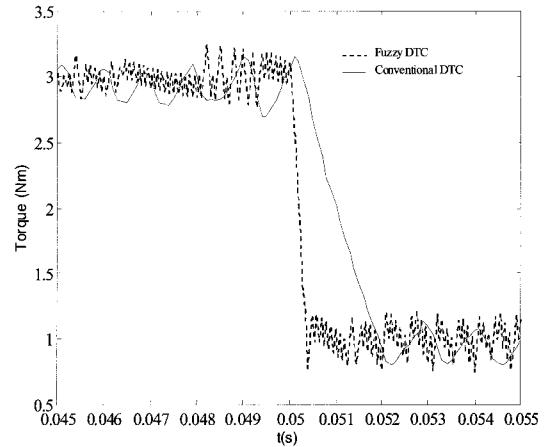


Fig. 14. Torque response of fuzzy controller and conventional DTC for step change in command torque

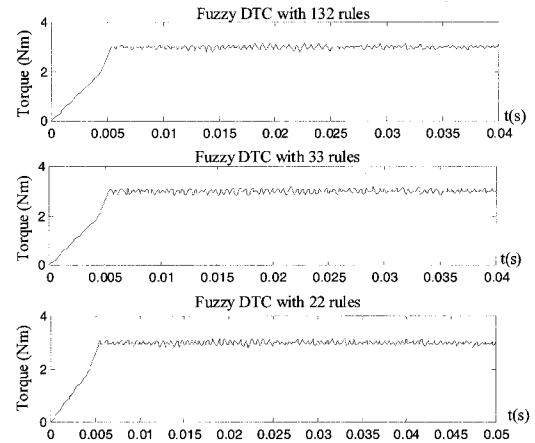


Fig. 15. Torque response of fuzzy controller for three approaches

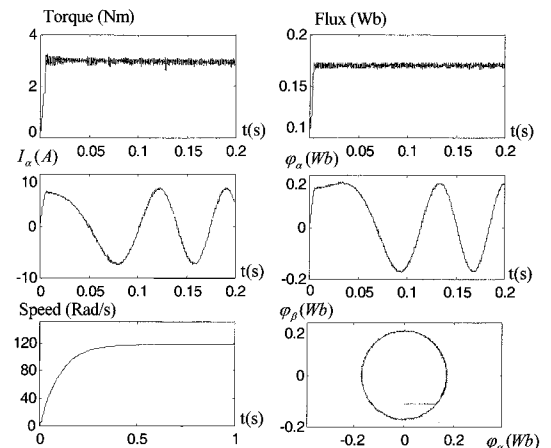


Fig. 16. Responses of the PMSM with the proposed approach

5. Fuzzy Resistance Estimator

In direct torque control schemes, estimation of stator flux is based upon the knowledge of stator resistance. This is especially true at low speeds where the resistive drop ($I_s R_s$) is the major portion of the measured terminal voltage. The stator resistance error would cause improper flux estimation making the controller perform poorly. The magnitude of the stator current vector can be used to correct the stator resistance used by the controller during any change in stator resistance of the machine. The magnitude of the stator current vector in direct self-control is a function of torque and flux. It is not affected by any change in the input DC voltage or a change in load. Also, the model used in the direct self-controller is independent of all machine parameters other than stator resistance. Change of any parameter other than stator resistance does not change the magnitude of the stator current vector. For any change in the current vector, during a change in the input voltage or the motor parameters other than stator resistance, the controller chooses the switching states so that the stator current changes back to its original value to have constant flux and torque [16]. During a change in stator resistance the actual and the estimated stator flux are different. Therefore, the switching states selected by the controller for constant flux and torque do not change the current to its constant value. Thus, for a constant value of torque and stator flux, any change in the magnitude of the stator current vector is due to the change in stator resistance. With knowledge of the magnitude of current vector, for the given values of stator flux and torque, a fuzzy resistance estimator can be developed for the correction of changes in stator resistance. The fuzzy resistance estimator suggested is shown in Fig. 17. The estimator requires the magnitude of the stator current vector to obtain the change in stator resistance. This magnitude is obtained by measuring the stator currents and calculating the current vector. This is filtered and sent to the fuzzy resistance estimator.

To estimate the error in stator resistance, the stator current vector error and the change in the current vector error are employed. The current vector error and the change in current vector error are defined as:

$$\begin{aligned} e(k) &= I_s^*(k) - I_s(k) \\ \Delta e(k) &= e(k) - e(k-1) \end{aligned} \quad (17)$$

Where $I_s^*(k)$ is the current vector corresponding to the flux and torque commands and $I_s(k)$ is the measured stator current vector given by:

$$I_s(k) = \sqrt{i_\alpha^2 + i_\beta^2} \quad (18)$$

The universe of discourse of the two fuzzy input variables

and the output variable, which is the change in stator resistance, ΔR_s are divided into five fuzzy sets each as shown in Fig. 19.

The fuzzy rule applied can be written as:

$$R_i : \text{if } e \text{ is } A_i \text{ and } \Delta e \text{ is } B_i \text{ then } \Delta R_s \text{ is } C_i \quad (19)$$

The error in the stator current vector for a linear change in stator resistance is shown in Fig. 19., shows the relation between the error in the stator current vector and the error in stator resistance. Using this response we can formulate fuzzy

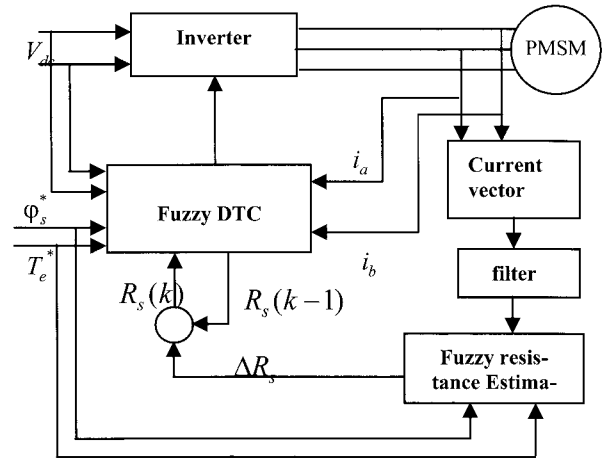


Fig. 17. Fuzzy DTC Controller with fuzzy resistance estimator

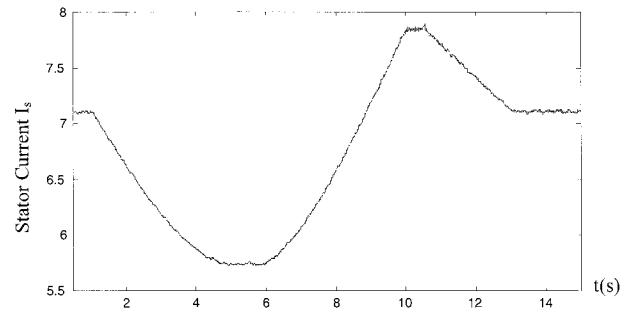


Fig. 18. Error in stator current for linear change in stator resistance

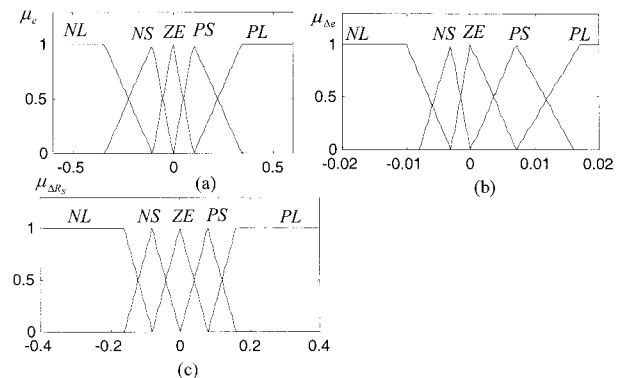


Fig. 19. Membership distribution of fuzzy input and output variables

Table 11. Fuzzy rules for fuzzy resistance estimator

$e/\Delta e$	PL	PS	ZE	NS	NL
PL	PL	PL	PL	PS	ZE
PS	PL	PL	PS	ZE	NS
ZE	PL	PS	ZE	NS	NL
NS	PS	ZE	NS	NL	NL
NL	ZE	NS	NL	NL	NL

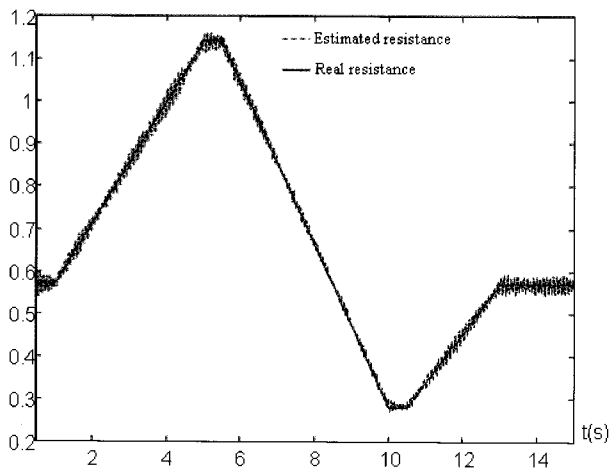
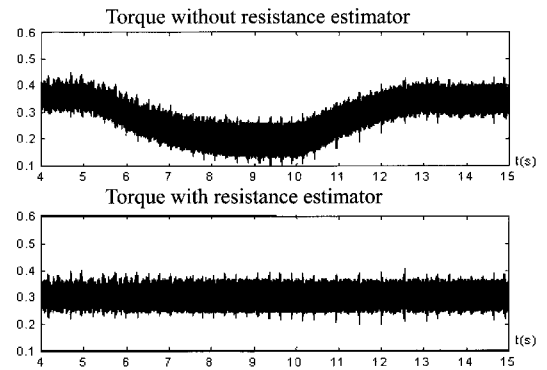
rules to change the stator resistance used by the controller. There are 25 rules as shown in Table 11. Mamdani's minimum operation rule is used as the interface method and, finally, the value of resistance error can be obtained by the center of gravity method used for defuzzification. The value of stator resistance used by the controller is then given by:

$$R_s(k) = R_s(k-1) + \Delta R_s \quad (20)$$

5.2 Simulation Results

The stator resistance variation was simulated as well. The speed of the PMSM is set at 4 rad/s and torque reference 0.3 Nm. The stator resistance used by the controller follows very closely the actual stator resistance of the motor, and the simulation results are shown in Fig. 20.

Fig. 21 shows the filtered electric torque with and without the fuzzy resistance estimator. There is very small error in actual electric torque of the machine during a change in resistance using the fuzzy resistance estimator.

**Fig. 20.** Fuzzy resistance estimator**Fig. 21.** Torque response with and without fuzzy resistance estimator

6. Conclusion

A fuzzy logic controller using the DTC strategy for PMSM has been described in this paper. To make the fuzzy reasoning fast and the simulation available with the fuzzy logic toolbox, the number of rules was greatly reduced in terms of the flux angle mapping approach. The change in the steady state value of stator current for a constant torque and flux reference is used to change the value of stator resistance used by the controller to match the machine resistance. The simulation results show the effectiveness of the new control strategies.

References

- [1] L. Tang, L. Zhong and F. Rahman, "Modelling and Experimental Approach of a Novel Direct Torque Control Scheme for Interior Permanent Magnet Synchronous Machine Drive", in *Proceedings of IEEE IECON 02 28th Annual Conference*, pp.235-240, 5-8 Nov. 2002.
- [2] I. Takahashi and T. Noguchi, "A New Quick-Response and High-Efficiency Control Strategy of an Induction Motor", *IEEE Trans. Industrial Application*, vol.IA-22, no.5, pp.820-827, Sept/October 1986.
- [3] L. Zhong and M. F. Rahman, "Analysis of Direct Torque Control in Permanent Magnet Synchronous Motor Drives", *IEEE Trans. Power Electronics*, vol.12, no.3, pp.528-535, May 1997.
- [4] M. F. Rahman and L. Zhong, "A Direct Torque Controller for Permanent Magnet Synchronous Motor Drives", *IEEE Trans. Energy Conversion*, vol.14, no.3, pp.637-642, Sep. 1999.
- [5] M. F. Rahman and L. Zhong, "A Direct Torque-Controlled Interior Permanent Magnet Synchronous Motor Drive Incorporating Field Weakening", *IEEE Trans. Industrial Application*, vol.34, no.6, pp.1246-1253, Nov./Dec. 1998.
- [6] M. R. Zolghadri, *Contrôle Direct du Couple des Actionneurs Synchrones*: Phd Thesis, INP Grenoble, France 1997.
- [7] Y. Lai and J. Chen, "A New Approach to Direct Torque

- Control of Induction Motor Drives for Constant Inverter Switching Frequency and Torque Ripple Reduction”, *IEEE Trans. Energy Conversion*, vol.16, no.3, pp.220-227, Sep. 2001.
- [8] S. A. Mir and D. S. Zinger, “Fuzzy Implementation of Direct Self Control for Induction Machines”, *IEEE Trans. Industrial Application*, vol.30, no.3, pp.729-735, May\Jun. 1994.
- [9] K. Benmansour, H. Rezine and M.S. Boucherit, “Nouvelle approche de la commande floue base sur DTC de la machine synchrone a aimant permanent”, *CIFA*, Tunisie, July 2004.
- [10] J. Liu, P. Wu and H. Xiping, “Application of Fuzzy Control in Direct Torque Control of Permanent Magnet Synchronous Motor”, *Proceeding of 5th world congress on intelligent Control and automation*, Hangzhou, China, June 2004.
- [11] M. Fu and L. Xu, “A Sensorless Direct Torque Control Technique for Permanent Magnet Synchronous motors”, in *Proceedings of IEEE Power Electronics in Transportation*, pp.21-27, 22-23 Oct. 1998.
- [12] M. F. Rahman and L. Zhong, “An Investigation of Direct and Indirect Torque Controllers for PM Synchronous Motor Drives”, in *Proceedings of IEEE PEDS'97 Conference*, Singapore, pp. 519-523, 26-29 May 1997.
- [13] D. Casadei, G. Grandi and G. Serra, “Effects of Flux and Torque Hysteresis Band Amplitude in Direct Torque Control of Induction Machines”, in *Proceedings of IEEE IECON'94 20th International Conference*, pp.299-304, 5-9 Sep. 1994.
- [14] G. Buja, D. Casadei and G. Serra, “Direct Stator Flux and Torque Control of Induction Motor: Theoretical Analysis and Experimental Results”, in *Proceedings of IEEE International Conference*, pp.T50-T64, 1998.
- [15] D. O. Neacsu, “Comparative Analysis of Torque-Controlled IM Drives with Applications in Electric and Hybrid Vehicles”, *IEEE Trans. Power Electronics*, vol.16, no.2, pp.240-247, March 2001.
- [16] S. A. Mir and D. S. Zinger, “Fuzzy Controller for Inverter Fed Induction Machines”, *IEEE Trans. Industrial Application*, vol.30, no.1, pp.78-83, Jan.\Feb. 1994.
- [17] B. K. Bose, L. Fellow, “Quasi fuzzy Estimation of Stator Resistance of Induction Motor”, *IEEE Trans. Power Electronics*, vol.13, no.3, pp.401-408, May 1998.
- [18] H. Rezine and A. Derbane, “Implémentation du Contrôle Direct du Couple de la Machine Synchrone à Aimants Permanents par la Logique Floue”, *International Conference CGE'02*, Algiers EMP, Algeria, 2002.
- [19] T. Noguchi, K. Yamada, S. Konodo and I. Takahashi, “Initial Rotor Position Estimation Method Sensorless PM Synchronous Motor with no Sensitivity to Armature Resistance”, *IEEE Trans. Industrial Application*, vol.45, no.1, pp.118-124, Feb. 1998.
- [20] S. Mir, E. Malik, D. S. Zinger, “PI and Fuzzy Estimation for Tuning the Stator Resistance in Direct Torque Control of Induction Machines”, *IEEE Trans. Power Electronics*, vol.13, no.2, pp.279-287, March 1998.
- [21] Y. Xia, W. Oghanna, “Fuzzy Direct Torque Control of

Induction Motor with Stator Flux Estimation Compensation”, in *Proceedings of IEEE IECON'97 23rd International Conference*, pp.505-510, 9-14 Nov. 1997.



Abdelhalim Tlemcani

He received his engineering degree and M.Sc. in power electronics from the National Polytechnic School of Algiers (ENP), Algeria, in 1997 and 1999, respectively. He received his Ph.D. degree in electrical engineering from ENP in 2007. Since 2002 he has held teaching and research positions in

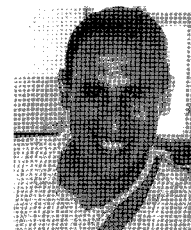
the Department of Electrical Engineering, UYFM, where he is currently Associate Professor. He is member of Process Control Laboratory. His research interests are in electrical drives, power electronics, robust and nonlinear control and fuzzy systems.



Ouahid Bouchhida

He received his ‘Ingénieur d’Etat’ degree (equiv. BSc.+one year) in Electrotechnics and ‘Magister’ degree (equiv. MPhil) in electrical engineering from the ‘Ecole Nationale Polytechnique, Algiers, Algeria, in 1995 and 1998 respectively. He received his Ph.D. degree in electrical engineering from

ENP in 2008. Since 1999 he has held teaching and research positions in the Department of Electrical Engineering, UYFM, where he is currently Assistant Professor. His current research interests are integrated actuators, machine speed sensors and drives.



Khelifa Benmansour

He received his Engineer degree in Electrotechnics, and Magister degree in electrical engineering, from the Ecole Nationale Polytechnique, (ENP, EMP) Algiers, Algeria, in 1997, 1999 respectively. He received his Ph.D. degree in electrical engineering from ENP in 2006. He is a member of the

ECS research group, ENSEA, His current research interests are integrated actuators, machine speed sensors, drives, multicells inverter and hybrid system.

**Djamel Boudana**

He received his Engineer degree in Electrotechnics, and Magister degree in electrical engineering, from USTHB Algiers, Algeria, in 1995 and 1999 respectively. Since 2001 he has held teaching and research positions in the Department of Electrical Engineering, UYFM, where he is currently Assis-

tant Professor. He is a member of Process Control Laboratory. His research interests are in electrical drives.

**Mohamed Seghir Boucherit**

He received his Engineer degree in Electrotechnics, the Magister degree and the Doctorat d'Etat (Ph.D. degree) in electrical engineering, from the National Polytechnic School, Algiers, Algeria, in 1980, 1988 and 1995 respectively. Upon graduation, he joined the Electrical Engineering Department

of National Polytechnic School. He is a Professor, a member of Process Control Laboratory and his research interests are in the area of electrical drives and process control.